ELSEVIER

Chemical Engineering Journal 73 (1999) 229–245

Chemical Engineering Journal

Pressure drop modelling for liquid feed direct methanol fuel cells Part II. Model based parametric analysis

P. Argyropoulos*, K. Scott, W.M. Taama

Chemical and Process Engineering Department, University of Newcastle upon Tyne, Merz Court, Newcastle upon Tyne NE1 7RU, UK

Received 17 August 1998; received in revised form 9 February 1999; accepted 14 February 1999

Abstract

A pressure drop model for the direct methanol fuel cell (DFMC), described in Part 1 of this contribution, based on the homogeneous two-phase flow theory and mass conservation equation, which describes the hydraulic behaviour of a large (272 cm^2) cell, is used in a parametric analysis. The model allows assessment of the effect of operating parameters (temperature gradient, current density, flow bed design, fuel and oxidant flow rates and pressure) on the pressure losses at the anode and cathode side of the cell. The model is applied to an existing flow bed design, based on a plate heat exchanger, used in current fuel cell scale up studies. The role of the flow bed design is examined by presenting the pressure drop contributions for each of the three sections that comprise the flow bed.

Keywords: Direct methanol fuel cell; Pressure drop; Modelling; Stacks; Two-phase flow

1. Introduction

Direct methanol fuel cell (DMFC) stacks are still under development at a number of research groups world wide [1–8]. There are a number of scientific and technological issues yet to be solved with the DMFC, and most concern electrochemical problems associated with methanol oxidation, e.g. more active and cheaper electrocatalysts, methanol crossover through Nafion® 117 membranes etc., where the research effort has focused on improving the electrochemical performance of these cells [9–15]. However, there are also important engineering design aspects that remain to be studied, that have been mainly neglected. One of these is the fluid mechanic and pressure drop behaviour of DMFC. This behaviour determines the requirements for auxiliary equipment to operate the fuel cell stack and also has some bearing on the actual electrochemical performance of the fuel cell. This feature relates to the influence of methanol crossover in the cell, the generation of carbon dioxide gas, the vaporisation of methanol, and of water, from the cell streams and eventually to the hydraulic connection of cells in a large scale stack. A sound knowledge and understanding of how the operating and system parameters affect the cell behaviour will be a valuable source of information on deciding the system characteristics.

Part I of this paper described the model of the fuel cell in detail, while here, in Part II, we discuss and describe in detail the pressure drop characteristics.

2. Parametric analysis methodology

We have recently presented experimental results for DMFC system optimisation based on the effect of operation conditions on single cells performance [16,17]. Using the conclusions of those studies a number of operating parameters are selected to assess their effect on hydraulic behaviour in both the anode side and cathode side of the cell. A base case scenario is selected for each side of the cell, based on the most common operating conditions for a fuel cell of that type with a nominal active area of 272 cm^2. For the anode side these are: 1.0 $dm^3\ min^{-1}$ methanol solution flow rate, 2.0 M methanol concentration, 80°C solution inlet temperature, 4°C anode side total gradient, a current density of 100 mA cm^{-2}. In the case of the cathode side these are 2.0 barg cathode pressure, 22°C air inlet temperature, 40°C total cathode-side temperature gradient, and 2.0 $dm^3\ min^{-1}$ air flow rate.

The flow rates selected are equivalent to Reynolds numbers in the channels, assuming single-phase flow for anode

*Corresponding author.

1385-8947/99/$ – see front matter
PII: S1385-8947(99)00039-X

aqueous methanol solution and cathode air, of 186 for anode side and 12 for cathode side. It should, however, be remembered that in cell operation the flow is in fact two-phase in both side of the cell. For example, in the case of the anode with a current density of 100 mA cm^{-2}, as the methanol solution flow rate is changed between say 0.05 and 30 dm^3 min^{-1} the theoretical volumetric fraction of carbon dioxide, based on a 100% Faradaic production, in the outlet stream varies from approximately 0.60–0.0025. As will be shown, these variations will have a significant effect on the cell hydraulic behaviour.

The operating range to be used in our cell stack and economic considerations of the overall process dictate the range of parameters investigated in this work.

3. Anode side parametric analysis

The equation that is used to calculate the pressure drop in the anode side of the cell has four components:

$$\Delta p = \int_0^{l_l} \left[G^2(y) \left[\frac{2(yf(y)+K_I)\upsilon_f(y)}{d_{H,ge}} \times \left(1+\frac{x_0(y)\upsilon_{fg}(y)}{2\upsilon_f(y)}\right) + (\upsilon_f(y)-\upsilon_{fl}(y)) + \upsilon_{fg}(y)x_0(y) \right] + \frac{gy}{\upsilon_{fg}(y)x_0(y)} \ln\left(1+x_0(y)\frac{\upsilon_{fg}(y)}{\upsilon_f(y)}\right) \right] dy \quad (1)$$

The first component denotes the frictional pressure drop for two-phase conditions, and the second one accounts for the acceleration of the liquid due to a change in the specific volume which produces a small pressure drop. The third component represents acceleration pressure drop for the two-phase flow, and the fourth the two-phase gravitational head.

At low flow rates (typically from 0.005 to 1.0 dm^3 min^{-1}) the gravitational force term dominates since friction losses are low due to the low Reynolds numbers ($Re \leq 200$). As the flow rate increases friction losses become more important. The term relating to the change in the liquid specific volume gives a small pressure drop (typically less than 0.5% of the total side pressure drop). The two-phase flow related term accounts for almost 2% of the total pressure drop, (typically from 0.005 to 1.0 dm^3 min^{-1}) and increases with an increase in the gas fraction (i.e. high current densities and low liquid flow rates) where the presence of carbon dioxide is dominant. As the flow rate increases above 1.0 dm^3 min^{-1}, the gas fraction is reduced significantly and hence this associated term becomes very small.

The flow-bed design used in the cell stack is comprised of three parts, (i) a triangular shaped inlet section, (ii) the main flow-bed section, which is comprised of 57 identical parallel channels, and (iii) a second triangular outlet section. The two triangular sections typically account for less than 2–3% of the overall pressure losses at low flow rates ($\leq$1.0 dm^3 min^{-1}). With increasing liquid flow rate the pressure drop of the triangular outlet increases, but remains below 3% of the total pressure drop. This small pressure drop is somewhat misleading since the hydraulic resistance of the spots could be significant especially in the case of elevated flow rates. But as we have already explained such a feature is not included in the present model. The current model is readily adapted to explore the influence of other geometric configurations and MEA support structures in fuel cell stack, which are currently under consideration in our research programme. We, however, restrict our analysis to the one flow bed design to illustrate the general utility of the model.

Figs. 1 and 2 show an overall view of the influence of current density and flow rate on the pressure drop characteristics. Clearly there is significant interaction between the two variables as altering one of the operating conditions can affect more than one component of the aforementioned Eq. (1). In order to assess the overall anode side pressure drop behaviour, the following operating parameters were studied: current density, methanol solution flow rate, methanol concentration, feed inlet temperature, gas fraction at the outlet of the cell and anode side overall temperature gradient, i.e. temperature change between inlet and outlet ports. The latter effect arises from the heat produced in the fuel cell due to the various electric resistances in the cell and the enthalpies of reaction.

3.1. Current density

As can be seen in Fig. 3 the effect of increasing the current density on the pressure drop depends upon the flow rate of methanol solution through the cell. Increasing the current density can result in either a reduction in overall pressure drop (for a flow rate below 4.0 dm^3 min^{-1}), or an increase in pressure drop (for flow rates of above 5.0 dm^3 min^{-1}). From Figs. 1 and 2 it is, however, apparent that there are distinct regions of cell pressure drop performance.

1. Low and medium range flow rates (below 4.0 dm^3 min^{-1}) pressure drop falls with increasing current densities. This trend can be attributed to the fact that increasing the current density results in a higher carbon dioxide evolution rate and, to a lesser extent, a higher liquid reactant consumption rate. The vertical orientation of the cell directs gas bubbles upwards, creating a positive buoyancy force that assists the upward movement of liquid-phase and hence reduces the friction losses. In addition the physical properties of the two-phase mixture are altered as there is a higher gas content in the flow bed and hence the pressure drop components that are dependant upon the two-phase fluid physical properties are reduced. It should be noted that the model for gas bubble flow is relatively simple and does not include aspects of bubble coalescence and bubble swarm behaviour.

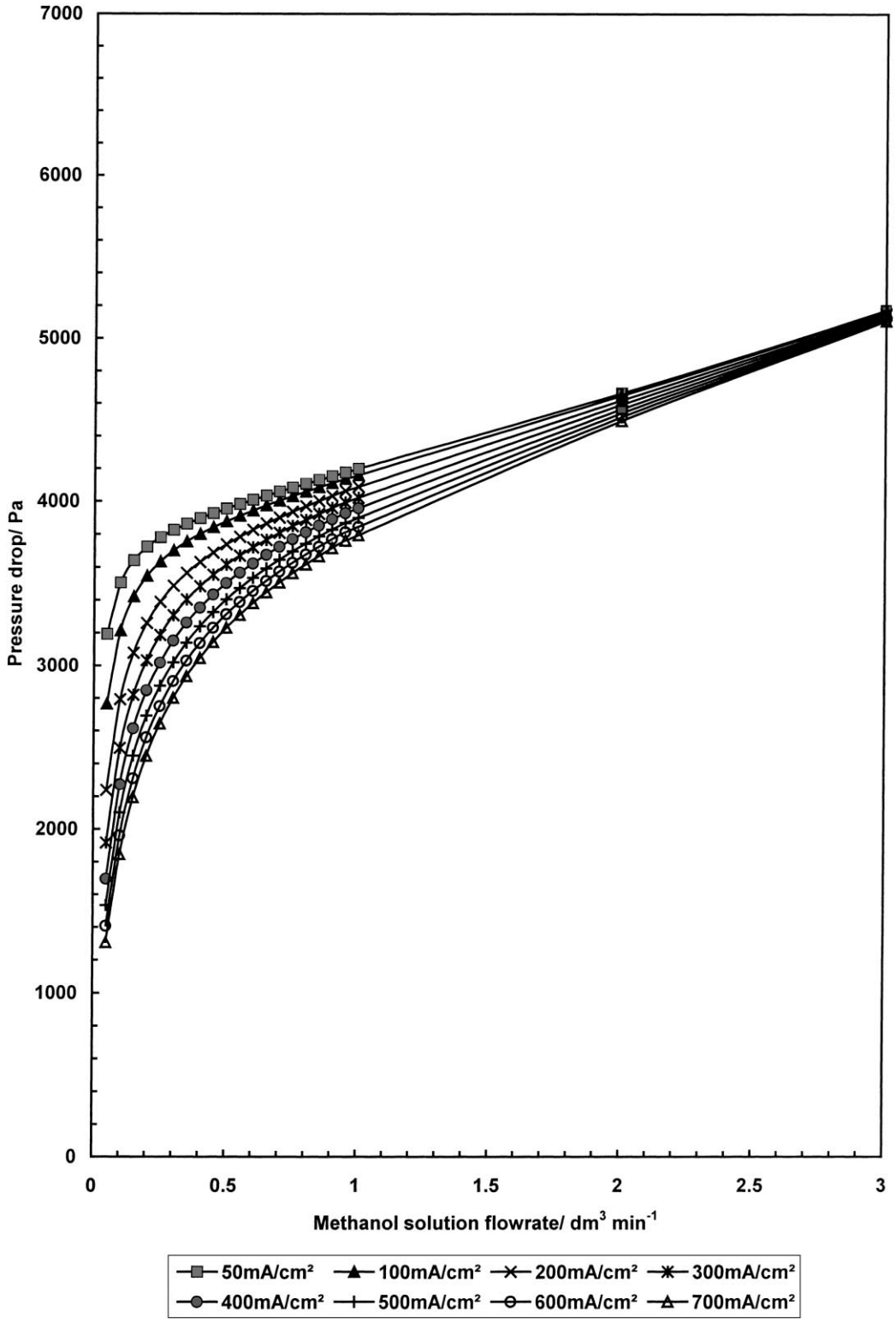

Fig. 1. Anode side pressure drop as a function of increasing current density (50–700 mA cm^{-2}) for low flowrates (0–3 dm^3 min^{-1}, 80°C cell temperature).

2. The higher flow rates increase the compartment's dynamic pressure and hence the gas is compressed, and the big bubbles or gas slugs are breaking down to form smaller size bubbles. At relatively high liquid flow rates the gas is present mainly as very finely dispersed bubbles. At low current densities the amount of gas is negligible and hence, with an almost single-phase liquid flow, the pressure drop continuously increases with increasing flow rate due to friction losses. The trend is followed for all the current densities.

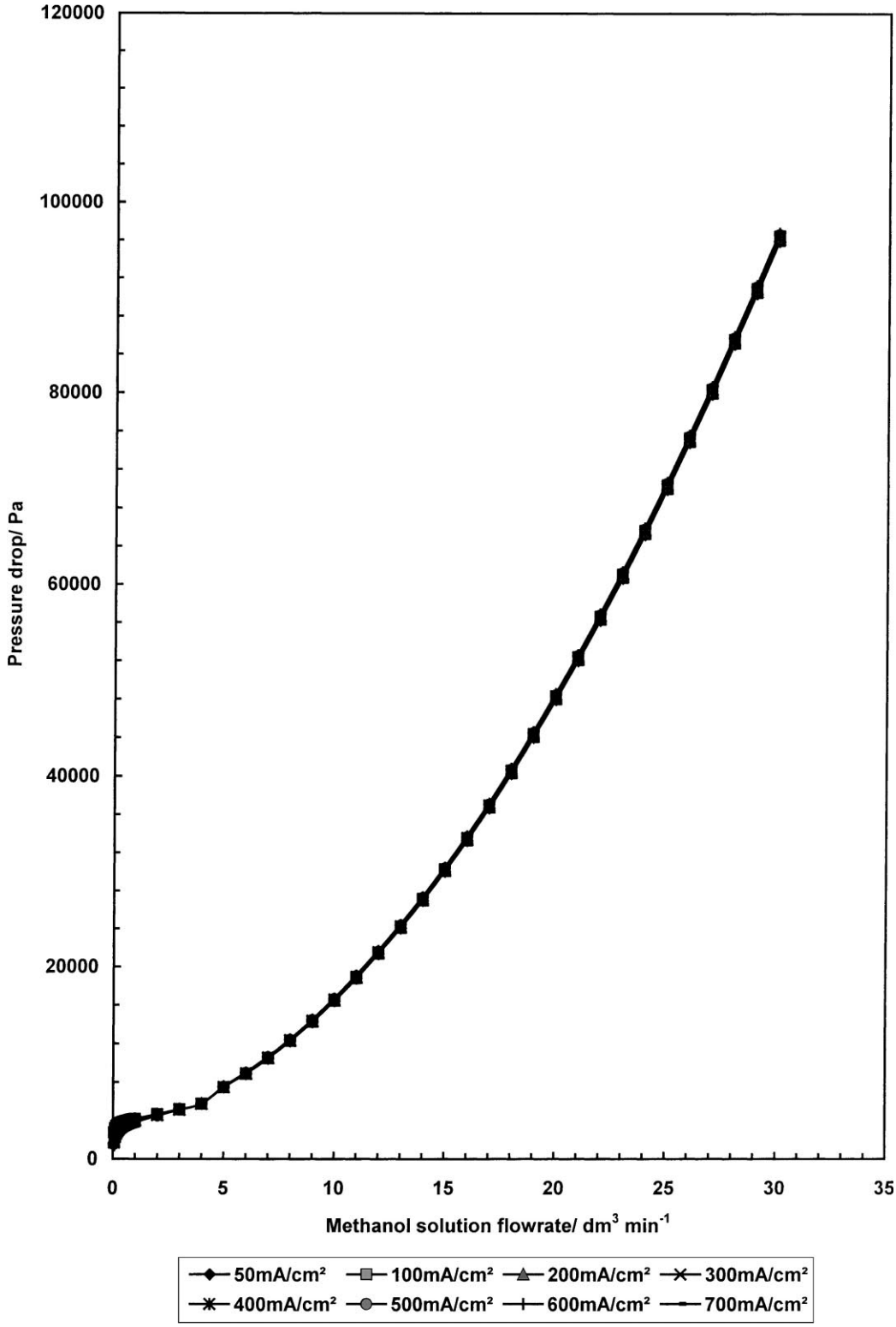

Fig. 2. Anode side pressure drop as a function of increasing current density (50–700 mA cm^{-2}) for medium-high flowrates (1–30 dm^3 min^{-1}, 80°C cell temperature).

3. At intermediate liquid phase flow rates (between approximately 3.0 and 4.0 dm^3 min^{-1}) the behaviour of the system shows the transition in the effect of current density on pressure drop. This is due to the dominant effect of pressure drop changing from a buoyancy derived influence to a frictional derived influence as identified above. This combination of phenomena- leads to a situation in which the pressure drop is almost

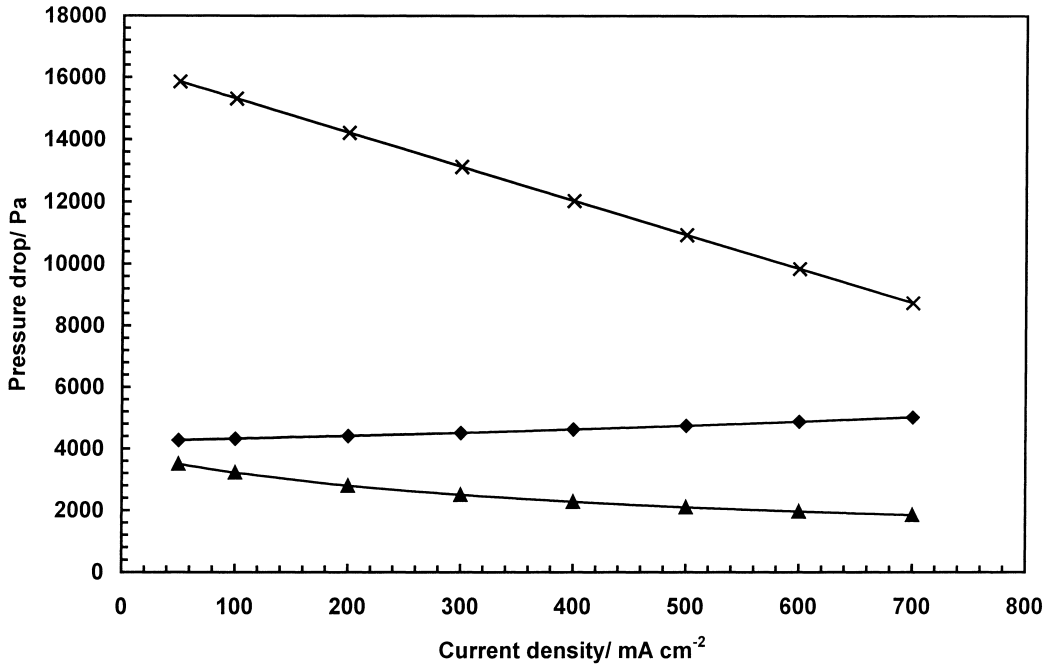

Fig. 3. Anode side pressure drop for increasing current density (50–700 mA cm^{-2}, anode side inlet flowrate 1.0 dm^3 min^{-1}, 80°C cell temperature).

constant and independent of the current density. At higher flow rates the behaviour is inverted and the presence of carbon dioxide only slightly affects the system behaviour. This is mainly due to the combination of two effects: (i) The increase in the volumetric flow rate of gas, which in turn increases the friction losses, (ii) the gas compression due to the high flow rates in use and hence the minimisation of the gas-lift which has the beneficial effect of reducing the pressure drop, as has already been explained.

3.2. Feed inlet flow rate

Methanol solution flow rate effects simultaneously the fuel conversion in the cell, the amount of carbon dioxide gas generated and also the methanol crossover through the membrane. All these factors influence the power generation capability of the cell. As shown in Fig. 4, increasing the feed inlet flow rate results in a significant increase in the overall pressure drop due to the increased fluid friction losses (higher local Reynolds number). At high flow rates the gas bubble fraction is small and thus there is a weak buoyancy related positive effect on pressure drop suppression. The effect of flow rate is severe at high flow rates (>5 dm^3 min^{-1}). For example the overall pressure drop is 3879 Pa for 0.5 dm^3 min^{-1} and 7457 Pa for 5.0 dm^3 min^{-1}, which represents a 92% increase.

3.3. Methanol solution concentration

Methanol solution concentration does not have a significant effect on the overall anode side pressure drop as shown in Fig. 5. Increasing methanol concentration reduces the pressure drop by a few Pascal, a change which is attributed to the change in the density and viscosity of the liquid phase, and the density-dependent physical properties of the two-phase fluid flowing in the anode flow bed.

3.4. Anode-side overall temperature gradient and feed inlet temperature

Fig. 6 shows the typical effect of temperature difference, between the inlet and the outlet ports, in the anode flow bed, on pressure drop. Increasing the anode side overall temperature gradient results in a small decrease in the overall pressure drop. The effect is more significant than for a change in methanol solution concentration since the temperature affects all the physical properties of the mixture. Nevertheless, this effect is still only of the order of a couple of hundred Pascal which is only a small fraction of the overall pressure drop.

As shown in Fig. 7, the feed inlet temperature has a noticeable effect on the anode side pressure losses. For a change of 10°C there is a reduction of approximately 200 Pa in the anode side pressure drop as a result in a change in the system physical properties. This though is still a considerably smaller effect than the two, dominant factors, of current density and inlet flow rate.

3.5. Outlet gas fraction

Essentially gas fraction is directly related to the operating current density due to the conversion of methanol to carbon dioxide. It is also affected by all the other operating

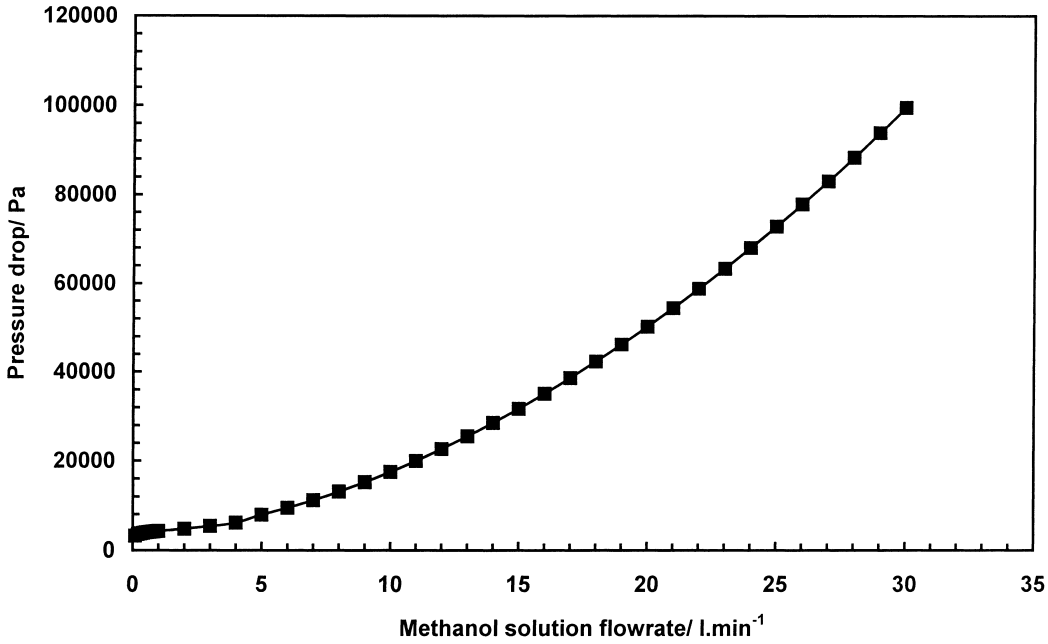

Fig. 4. Anode side pressure drop for increasing methanol solution flowrate (0.01–30 $dm^3\ min^{-1}$, 100 mA cm^{-2}, 80°C cell temperature).

parameters except probably methanol solution concentration. Gas fraction affects, to a large extent, the complex problem of anode side gas management and hence efficient carbon dioxide removal which is one of the issues that have to be solved prior to system commercialisation. Fig. 8 shows the anode side pressure drop as a function of increasing gas fraction for various flow rates. As can be seen, a 10% increment in the gas fraction can lead to 150 Pa reduction in the overall pressure drop. It should be noted that the gas fraction particularly affects the pressure drop behaviour at low liquid flow rates. However, even for a target flow rate of 1.0 $dm^3\ min^{-1}$ the influence of the gas presence cannot be neglected, as it is a critical factor, directly related to current density, that determines the cell's pressure drop behaviour.

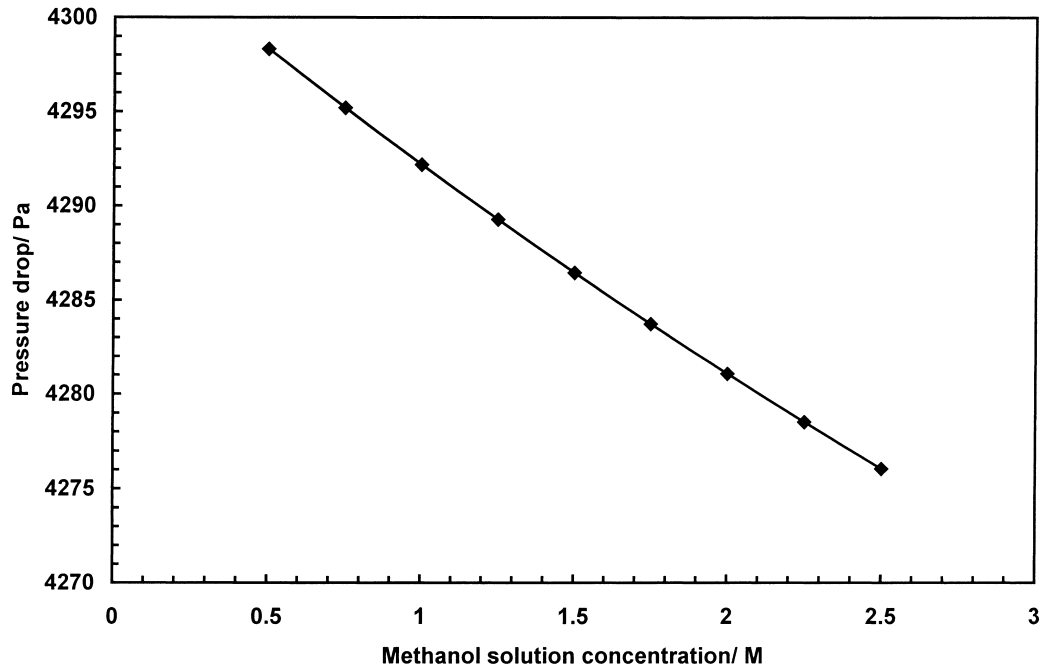

Fig. 5. Anode side pressure drop for increasing methanol solution concentration (0.5–2.5 M, inlet flowrate 1.0 $dm^3\ min^{-1}$, 100 mA cm^{-2}, 80°C cell temperature).

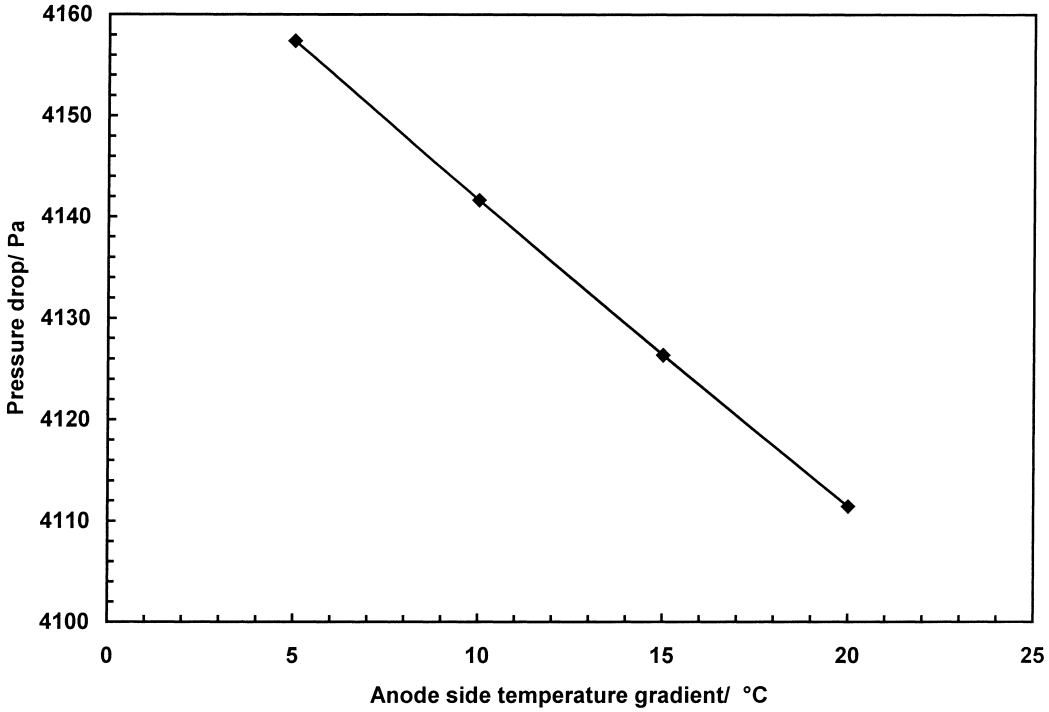

Fig. 6. Anode side pressure drop for increasing temperature gradient between inlet and outlet ports (inlet flowrate 1.0 $dm^3\ min^{-1}$, 100 mA cm^{-2}, 80°C cell temperature).

4. Cathode side parametric analysis

The equation that is used to calculate the pressure drop for the cathode side is:

$$\Delta p = \int_0^{l_l} \begin{cases} \left[G^2(y)\left[\dfrac{2(yf(y)+K_l)\upsilon_g(y)}{d_{H,ge}} + (\upsilon_g(y)-\upsilon_{gi}(y))\right] + \dfrac{gy}{\upsilon_{fg}(y)}\right]\mathrm{d}y \\ \left[G^2(y)\left[\dfrac{2(yf(y)+K_l)\upsilon_g(y)}{d_{H,ge}} \times \left(1+\dfrac{x_0(y)\upsilon_{fg}(y)}{2\upsilon_g(y)}\right) + (\upsilon_g(y)-\upsilon_{gi}(y)) + \upsilon_{fg}(y)x_0(y)\right] + \dfrac{gy}{\upsilon_{fg}(y)x_0(y)}\ln\left(1+x_0(y)\dfrac{\upsilon_{fg}(y)}{\upsilon_g(y)}\right)\right]\mathrm{d}y \end{cases} \quad (2)$$

The equation has to branches, the first represents the pressure drop for single phase flow, i.e. when there is no liquid water or methanol in the flow bed which is the case when the air is not fully saturated at the local conditions of temperature and pressure. The second branch has several terms. The first term of the second branch defines the frictional pressure drop for single phase and two-phase flow conditions, respectively. The second term accounts for the acceleration of the gas due to a change in the specific volume, which produces a small pressure drop. The third term represents acceleration pressure drop for two-phase flow. The fourth and the fifth terms denote single phase and two-phase gravitational head, respectively.

At low flow rates (less than 5.0 $dm^3\ min^{-1}$), the gravitational force related term dominates since friction losses are low at low Reynolds numbers. In addition with upward flow of air, an extra energy penalty is imposed from the work that required elevating the liquid droplets. As the flow rate increases the friction losses term becomes dominant. The higher air flow rate gradually reduces the amount of the liquid phase due to the increased quantities of liquid required to fully saturate the air stream. The term related to the change in the gas specific volume gives a small pressure drop (less than 0.5% of the total pressure drop). The two-phase flow related term accounts for almost 2% of the total pressure drop and increases in significance with an increase in the liquid fraction, i.e. higher operating current densities and lower flow rates.

The following operating parameters were studied for the cathode side: operating current density, air inlet flow rate, cathode side temperature gradient (i.e. temperature change between inlet and outlet ports), oxidant inlet temperature, and air inlet pressure. All these parameters are subject to variation in actual stack operation due to expected fluctuations in power demand.

4.1. Current density

As it can be seen in Figs. 9–11, increasing the current density results in a significant change in the overall pressure

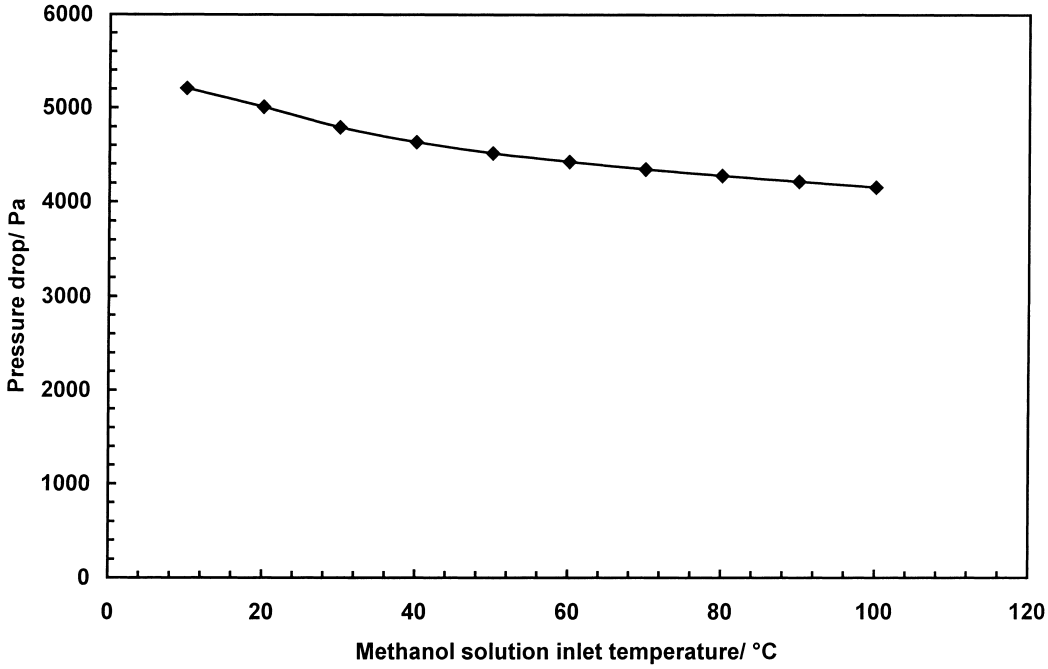

Fig. 7. Anode side pressure drop for increasing feed inlet temperature (10–100°C, inlet flowrate 1.0 dm^3 min^{-1}, 100 mA cm^{-2}, 80°C cell temperatue).

drop. At high air-flow rates, the pressure drop increases with current density due to an increase in the effective density and viscosity of the stream. This can be attributed to a higher water production rate at the catalyst layer and an increase in the water and methanol crossover through the membrane on increasing the current density. However, the amount of water and methanol needed to fully saturate the air depends on the temperature, pressure, flow rate and position in the

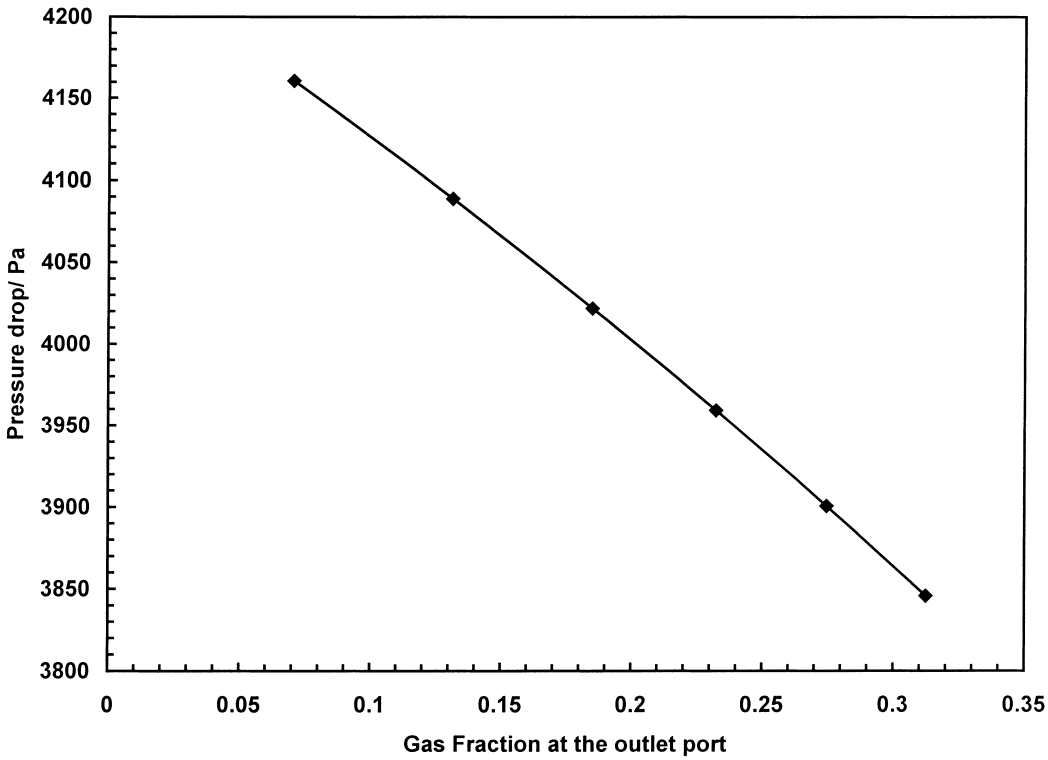

Fig. 8. Effect of outlet point gas fraction on the anode side pressure drop (inlet flowrate 1.0 dm^3 min^{-1}, 80°C cell temperature).

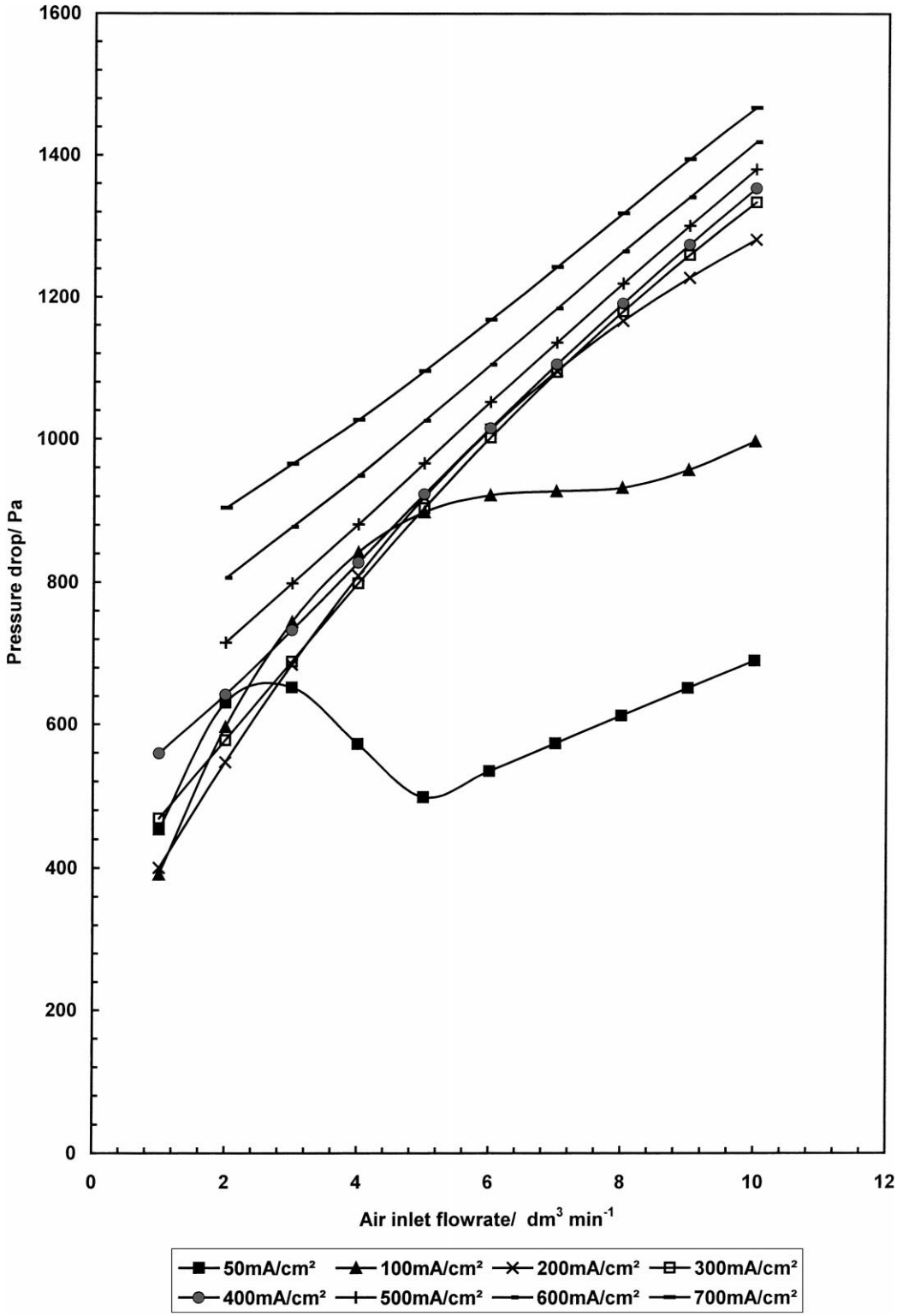

Fig. 9. Cathode side pressure drop as a function of increasing current density (50–700 mA cm^{-2}) for low and medium flowrates (1–10 dm^3 min^{-1}, 80°C cell temperature).

flow bed. Generally, as the fraction of liquid phase in the gas stream increases, then the cathode side pressure drop increases.

However, the aforementioned conclusion is not always valid. For example, in Fig. 9, at 50 mA/cm^2, there is initially a region where pressure drop increases with air inlet flow

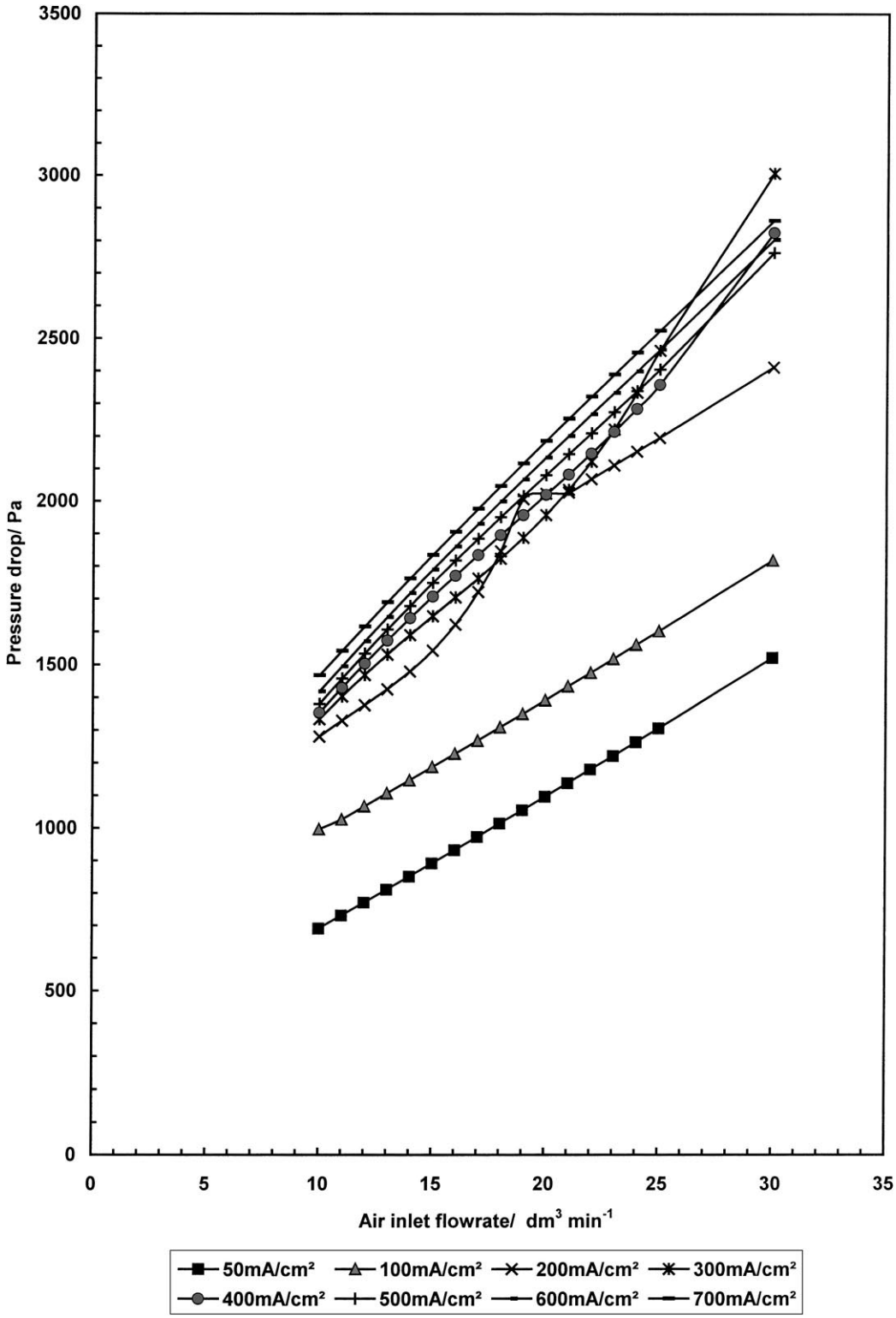

Fig. 10. Cathode side pressure drop as a function of increasing current density (50–700 mA cm^{-2}) for medium and high flowrates (10–30 dm^3 min^{-1}, 80°C cell temperature).

rate up to 2.0 dm^3 min^{-1}, followed then by a rapid decrease up to a flow rate of 5.0 dm^3 min^{-1}, and finally a third region where again pressure drop increases with air inlet flow rate but at a different rate to that in the other sections. The behaviour can be explained as follows: for low air flow rates there is a two-phase flow, with a fully saturated gas, and

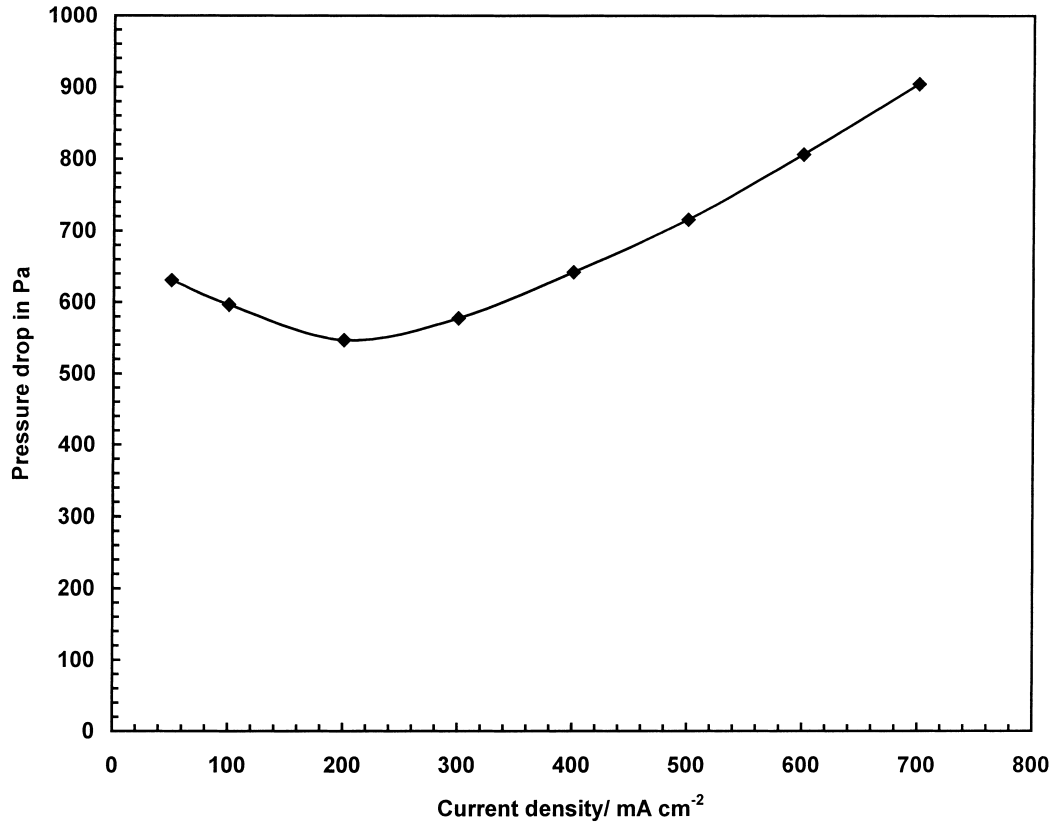

Fig. 11. Cathode side pressure drop for increasing current density (50–700 mA cm^{-2}, anode side inlet flowrate 1.0 dm^3 min^{-1}, 80°C cell temperature).

some liquid phase in the flow bed. As the flow rate increases, with the water production remaining the same (constant current density, i.e. constant water and methanol quantity at the cathode compartment), the liquid phase is not fully depleted by the air stream, but the amount of the liquid is constantly lowered (higher quantity of liquid is needed to reach the saturation point of a larger gas quantity) and hence the reduction in the pressure drop. Finally, with even higher gas flow rates the liquid phase becomes rapidly depleted and hence the pressure drop is a result of a purely gaseous flow, which is increasing linearly with the increase of the inlet air volumetric flow rate.

The same profile is noticeable in all current densities, but it is shifted towards higher air inlet flow rates as current density increases. This is expected as the behaviour is dependent upon the amount of liquid phase in the cathode side flow bed.

Another source of unusual behaviour is due to the different mechanisms associated with pressure drop performance in the case of single-phase and two phase flow. The model performs a check, locally, about the mode of operation (single or two-phase conditions) and alters the routine used. An extra characteristic is that the friction dependent terms are calculated differently for laminar or turbulent flow and these can result in localised increased pressure losses, which upset the smooth pressure drop profile.

4.2. Oxidant inlet flow rate

In a fuel cell stack oxidant flow must be sufficient to meet the demands for electrochemical reaction in the cell without causing a significant drop in power performance. The air-flow must also be sufficient to prevent cathode flooding by water, i.e. to evaporate the water produced, and to also act as a coolant for the cell to assist thermal management of the stack.

Increasing the oxidant/air inlet flow rate results in a significant increase in the overall pressure drop (Fig. 12). In the full range of oxidant flow rates investigated here the pressure loss increases gradually, depending on the operating current density. This is explained by a considerable liquid droplet formation in the flow and that the pressure drop due to the upward movement of the liquid is dominant in the low flow rate range. As the flow rate increases almost all the water is evaporated and single-phase flow prevails, with pressure losses attributed to increased friction. The rate of that increase in overall pressure drop depends on the current density, since this determines the rate of water generation in the cathode channel. The effect of flow rate on pressure drop is, for example, at a current density of 100 mA cm^{-2}, 391 Pa for 1.0 dm^3 min^{-1} and 996 Pa for 10 dm^3 min^{-1}, which represents a 60% increase for a ten-fold increase in flow rate. For higher oxidant flow rates the rate of increase in pressure drop with flow rate is greater, i.e.

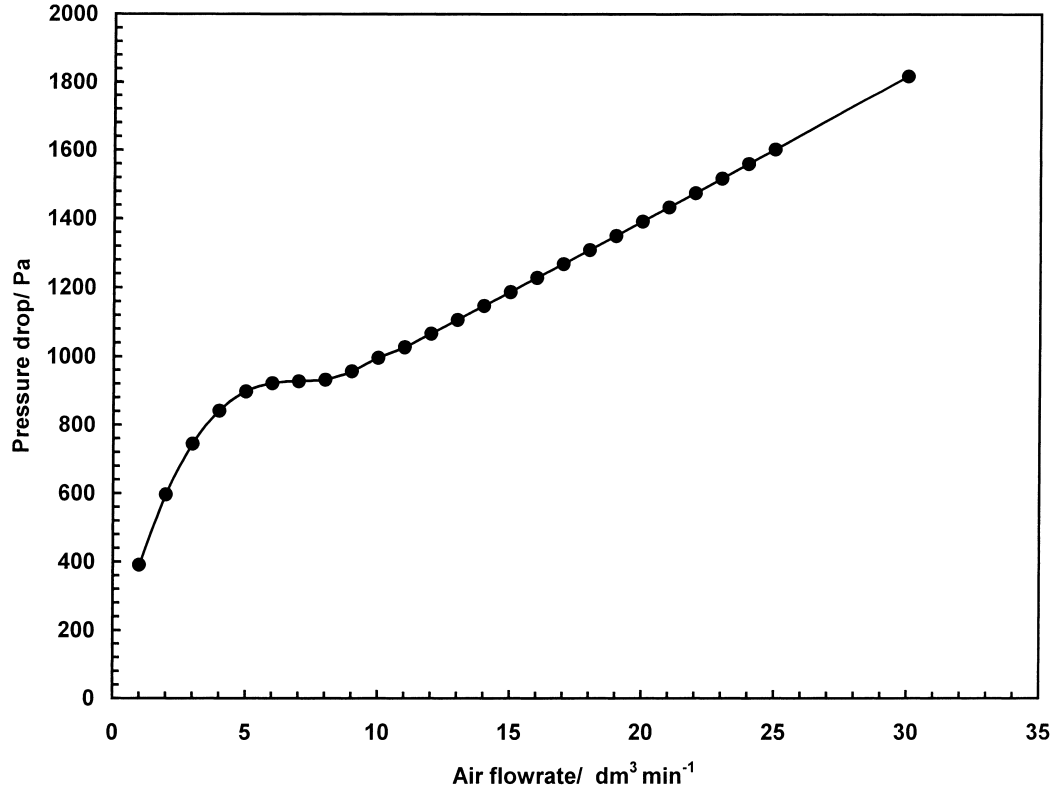

Fig. 12. Cathode side pressure drop for increasing air inlet flowrate (1–30 $dm^3\ min^{-1}$, 100 mA cm^{-2}, 80°C cell temperature).

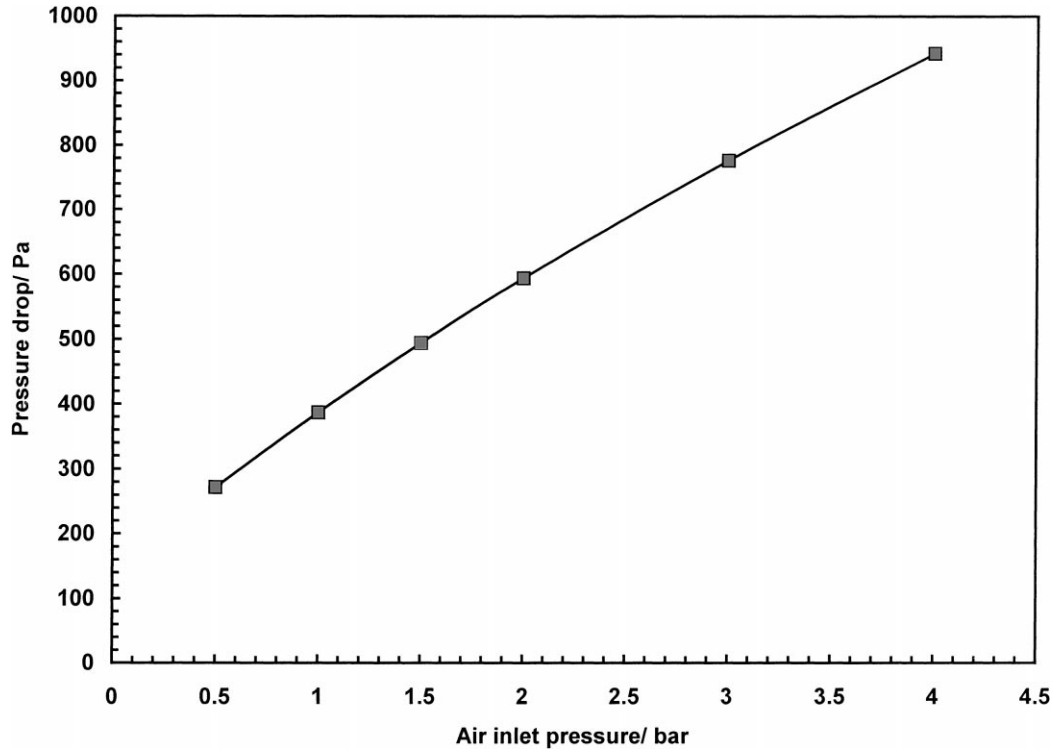

Fig. 13. Cathode side pressure drop for increasing cathodic compartment overpressure (0.5-4 bar, air inlet flowrate 1 $dm^3\ min^{-1}$, 100 mA cm^{-2}, 80°C cell temperature).

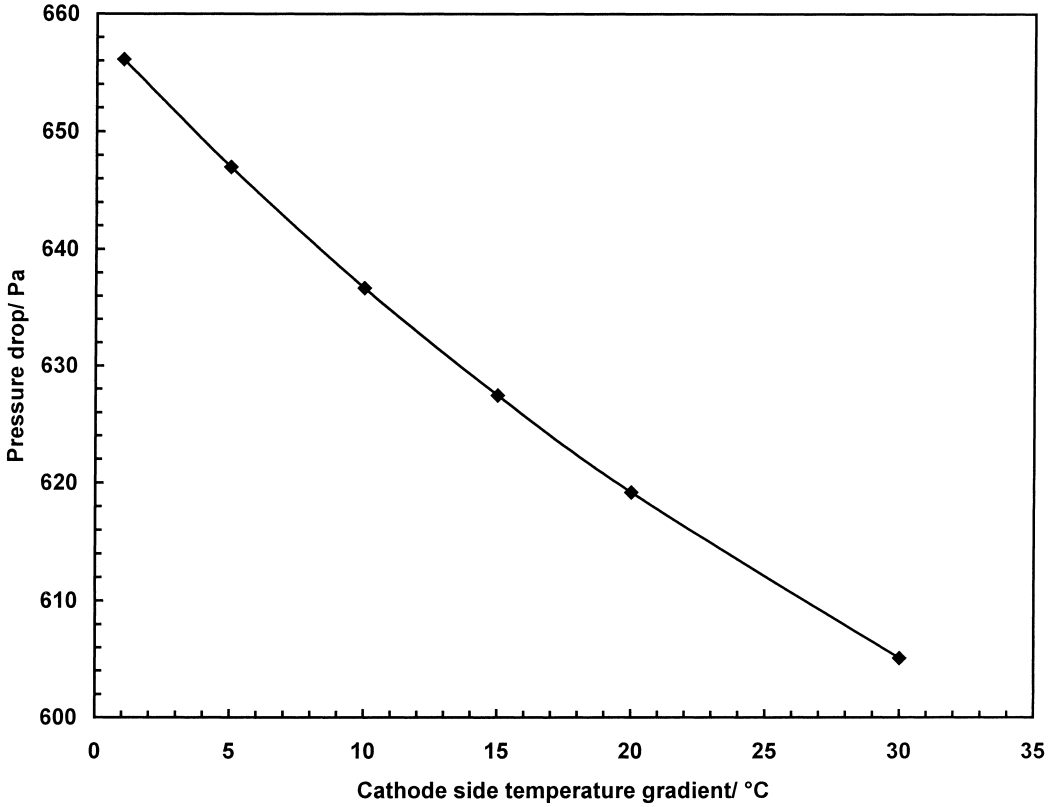

Fig. 14. Cathode side pressure drop for increasing temperature gradient between inlet and outlet ports (inlet flowrate 1.0 dm^3 min^{-1}, 100 mA cm^{-2}, 80°C cell temperature).

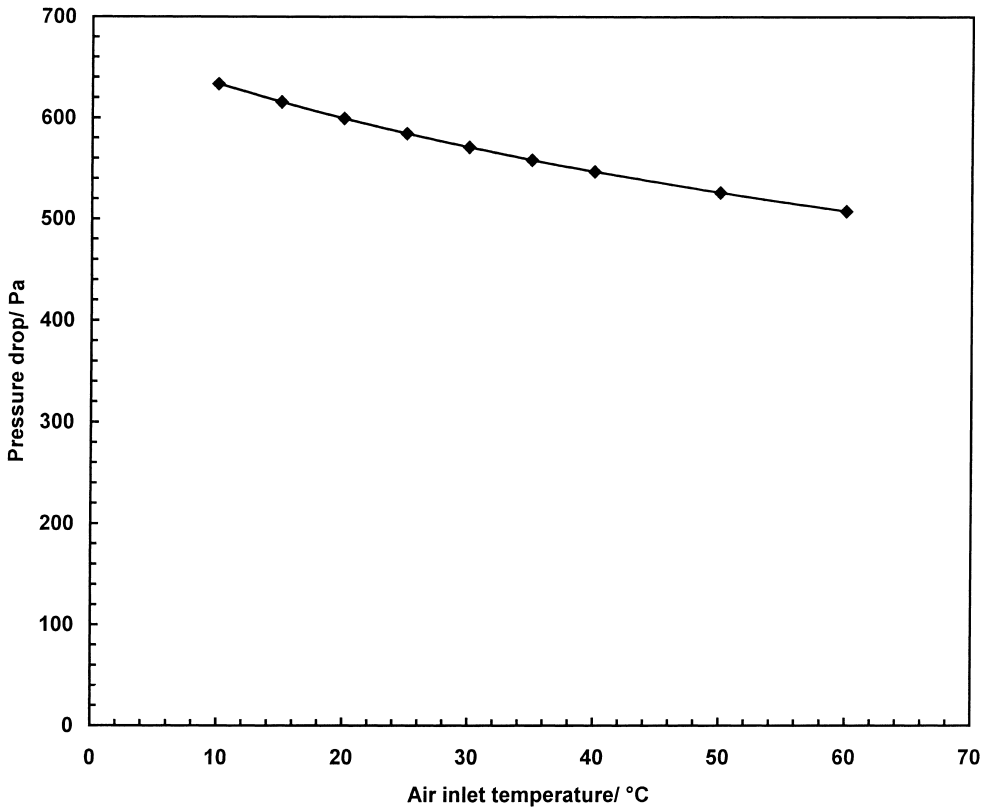

Fig. 15. Cathode side pressure drop for increasing air inlet temperature (10–60°C, inlet flowrate 1.0 dm^3 min^{-1}, 100 mA cm^{-2}, 80°C cell temperature).

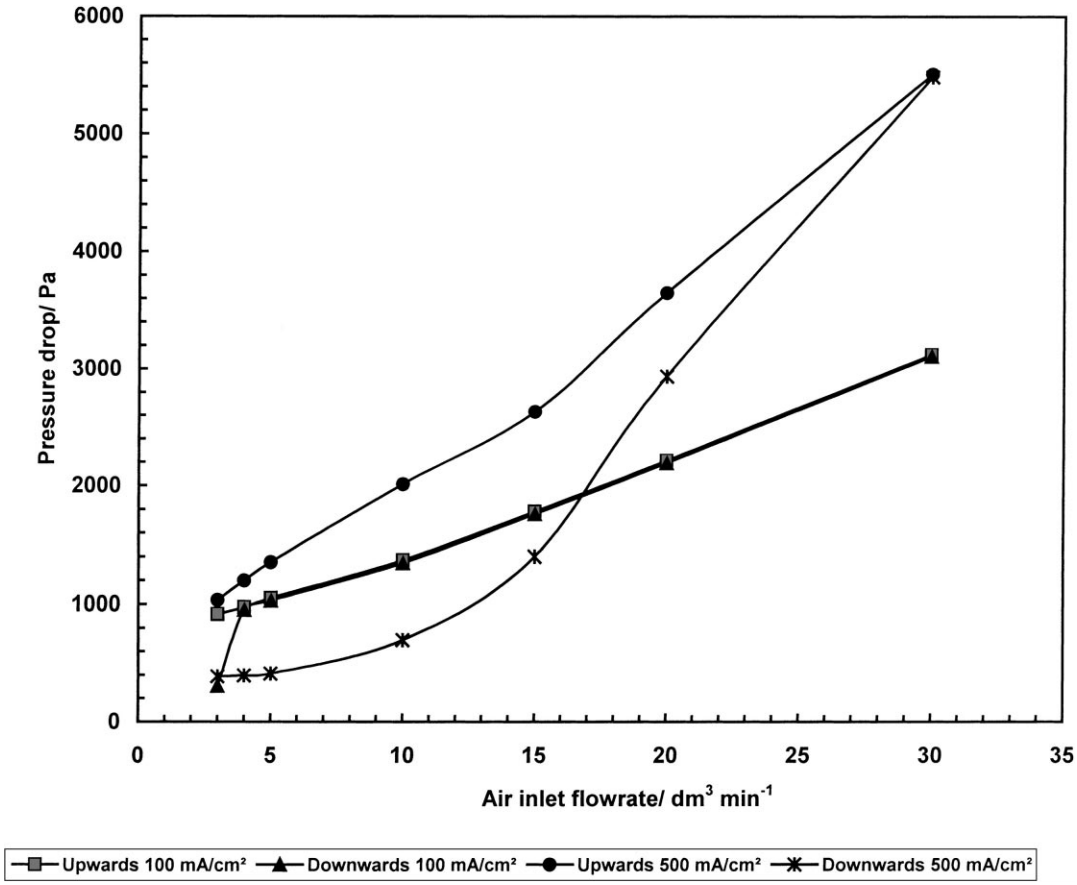

Fig. 16. Effect of cathode side flow orientation on pressure drop performance (inlet flowrate 1.0 $dm^3\ min^{-1}$, upwards and downwards 100 mA cm^{-2} and 500 mA cm^{-2}, 80°C cell temperature).

the pressure drop is 996 Pa for 10 $dm^3\ min^{-1}$ and 1817 Pa for 30 $dm^3\ min^{-1}$ an increase of 46% for a three-fold increment of the inlet flow rate.

4.3. Air inlet pressure

In the operation of a fuel cell, an advantage of pressured air is an increase in power performance due to an increase in oxidant supply and also a reduction in methanol crossover. The disadvantage of pressurised air is the increase in cost associated with its supply and use. The effect of air inlet pressure on the cathode side pressure drop is illustrated in Fig. 13. The significant increase in pressure drop can be attributed to an increase in the oxidant mass flow rate with increasing inlet pressure, with all the other parameters remaining constant. Hence, there is a greater contribution from friction in the pressure drop.

4.4. Cathode side overall temperature gradient

The temperature difference between the inlet and the outlet air in the cathode flow bed will vary depending upon the power output and thus resistive Joule heating, and reaction enthalpies. Fig. 14 depicts the effect of the temperature difference between the inlet and the outlet port of the cathode side flow bed on the cathode side pressure drop. Increasing the cathode side temperature gradient decreases slightly the overall pressure drop due to the effect of temperature on all the physical properties of the mixture. The effect is relatively small, of the order of a few hundred Pascal, and is only a small percentage (<10%) of the overall pressure drop.

4.5. Oxidant inlet temperature

The selection of oxidant inlet temperature to a stack depends on factors such as the required cooling in the cell, water removal, power performance, drying out of parts of the membrane and heat recovery and exchange in the fuel cell stack system. The oxidant temperature has a noticeable effect on the cathode side pressure loss. As can be seen in Fig. 15, for an increase of 10°C, there is a reduction in pressure loss of approximately 20 Pa. The principle reason again is that a change of 10°C in the mixture temperature has a significant effect on the system physical properties.

4.6. Flow orientation

A problem associated with PEFC is created by the difficulty in removing completely the water from the cathode

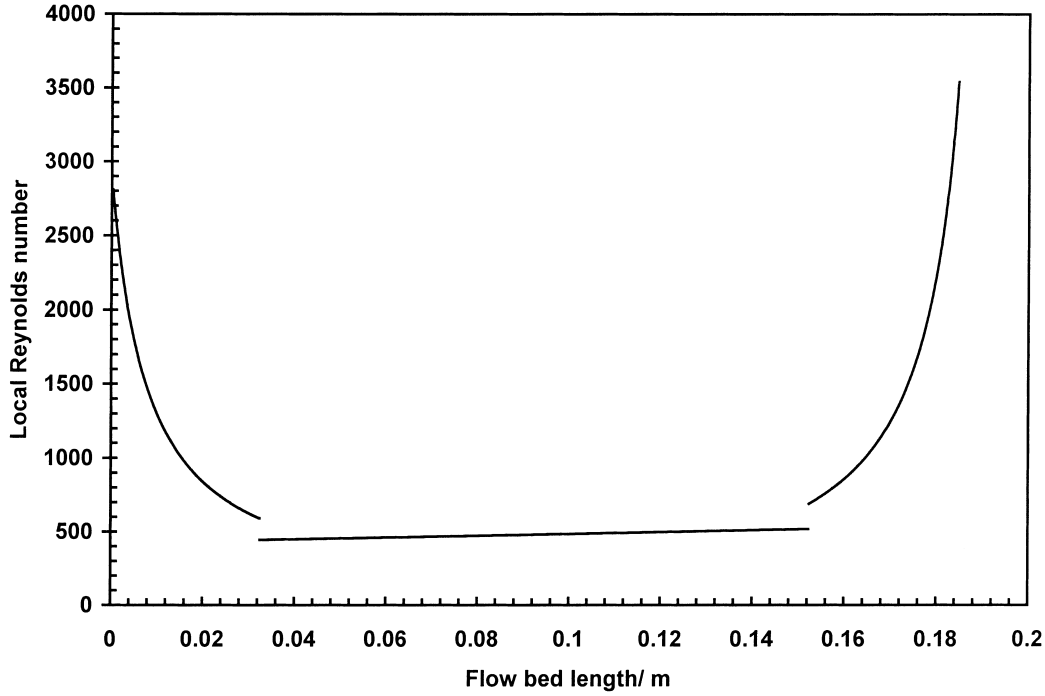

Fig. 17. Anode side local Reynolds number for increasing flow bed length (inlet flowrate 1.0 dm^3 min^{-1}, 100 mA cm^{-2}, 80°C cell temperature).

compartment. This results in possible cathode flooding and hence to performance deterioration, since the oxidant is not able to penetrate into the reaction sites. Making use of the gravitational force, by adopting a downwards cathodic flow configuration, helps to alleviate this problem. In addition due to the downward cathode side flow, the water droplets formed in the flow channels reduce the pressure drop as their cathodic movement is opposing to gas lift. In Fig. 16 we compare the two modes of operation, i.e. upward and downward flow. It is apparent that at a current density of 100 mA/cm^2 there is little difference in the resulting pressure drop with both orientations of flow. This is explained

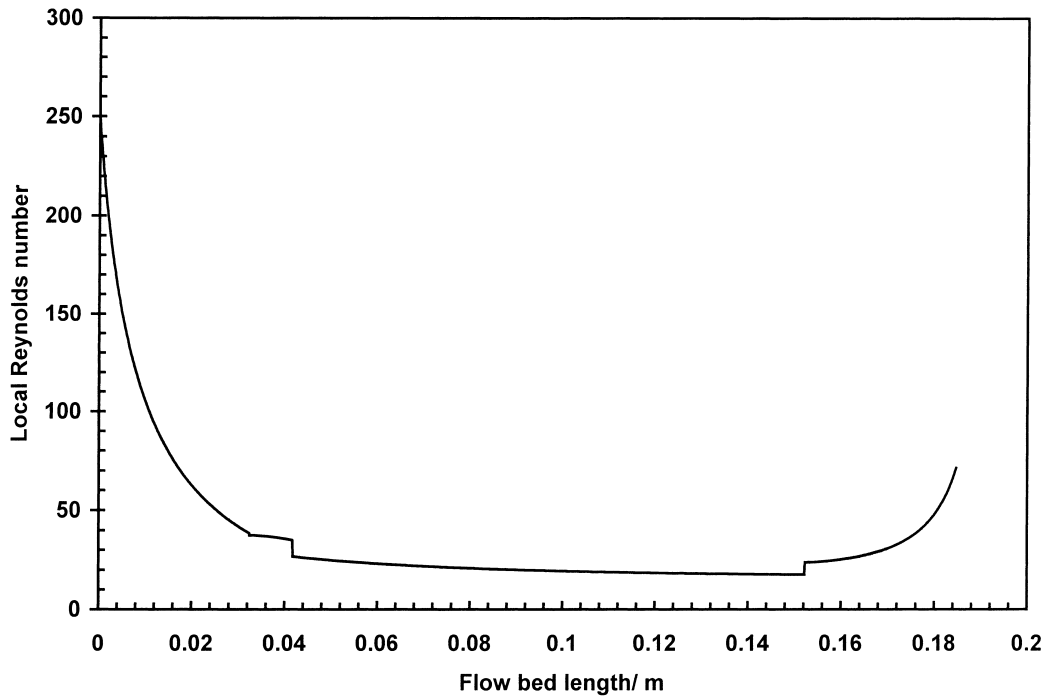

Fig. 18. Cathode side local Reynolds number for increasing flow bed length (inlet flowrate 1.0 dm^3 min^{-1}, 100 mA cm^{-2}, 80°C cell temperature).

from the small amount of liquid phase present in the flow channels. Increasing though the operating current density to 500 mA/cm^2 results in a significant pressure drop reduction, at least for low to medium range flow rates. As the flow rate increases the amount of liquid phase decreases and, as already explained, at some point the positive effect of the downward flow configuration is lost.

5. Local Reynolds numbers for the anode and cathode side

So far little information is available on the actual flow characteristics in both flow bed of the fuel cell. Figs. 17 and 18 show the Reynolds number profile for the whole vertical length of flow bed between the centres of the inlet and outlet ports. The Reynolds numbers are based on the physical properties of the two-phase mixture, the total local mass flow rate and the hydraulic diameter of the channel. As can be seen, depending on the operating conditions, the flow in the anode flow bed is a combination of turbulent flow at the region close to the inlet and outlet ports, and laminar in the remaining flow bed section. For the case of the cathode, the flow is laminar for low (as in Fig. 18) and medium flow rates and becomes a combination of turbulent and laminar flow, with turbulent flow at the region close to the inlet and outlet ports, and laminar at the remaining flow bed section for high flow rates and current densities.

6. Conclusions

A model is presented and used to assess the pressure drop performance of the anode and cathode side of a liquid feed DMFC cell with a flow bed design based on a plate heat exchanger concept. With the aid of the mathematical model an investigation of the effect of the full range of operating parameter on the pressure drop characteristics in both anode and cathode sides is presented.

For the case of the anode side, altering the inlet temperature, the methanol concentration or the overall anode side temperature gradient has a small effect on the overall pressure losses. On the contrary volumetric flow rate and current density have a more profound effect on pressure losses. In general increasing the flow rate increases the friction losses, while increasing current density reduces overall losses since it leads to the production of larger quantities of carbon dioxide gas.

Cathode side pressure losses are generally low, but not insignificant regarding practical fuel cell operation. This was expected since it is mainly a gas flow containing some dispersed droplets. Hence as the flow rate increases, and the amount of the liquid phase decreases, the losses are mainly due to friction. Increasing the current density, increases the resulting losses as, on one hand it leads to higher water and methanol crossover and an increased water production from the cathodic reaction, while on the other hand, it causes an increased oxygen consumption. Oxidant inlet temperature and overall cathode temperature gradient slightly reduce the pressure drop since the elevated temperatures increase the saturation point of air with water and methanol and hence reduce the amount of liquid in the flow bed. In addition they favour the physical properties of the gas mixture, i.e. a lower friction loss.

Overall the result of the analysis of pressure drop characteristics show that the critical parameters for estimating the pressure drop for each side of the cell are inlet stream fuel and oxidant flow rates and current density. The model has several functions which include sizing of auxiliary fuel cell equipment, predicting pressure drop behaviour of cell stacks, estimating pressure differentials between anode and cathode across the membrane and determining fuel cell performance locally as a function of pressure.

Acknowledgements

The authors would like to acknowledge the European Commission for supporting Mr P. Argyropoulos under a B20 TMR Marie Curie research training grant and, EPSRC for supporting Dr. W.M. Taama.

References

[1] S.R. Narayanan, G. Halpert, W. Chun, B. Jeffries-Nakamura, T.I. Valdez, H. Frank, S. Surampudi, The status of direct methanol fuel cell technology at JPL, in: 37th Power Sources Conference, Cherry Hill, NJ, USA, 1996.

[2] S.R. Narayanan, G. Halpert, W. Chun, B. Jeffries-Nakamura, T.I. Valdez, H. Frank, S. Surampudi, Recent advances in the performance of direct methanol fuel cells, in: Electrochemical Society Annual Meeting, Los Angeles, CA, USA, 1996.

[3] S.R. Narayanan, T. Valdez, N. Rohatgi, W. Chun, G. Halpert, Design of direct methanol fuel cell systems, in: 1998 Fuel Cell Seminar, Palm Springs, CA, USA, 1998.

[4] K. Scott, W.M. Taama, J. Cruickshank, Performance and modelling of a direct methanol solid polymer electrolyte fuel cell, J. Power Sources 65 (1-2) (1997) 159–171.

[5] K. Scott, W.M. Taama, J. Cruickshank, Performance of a direct methanol fuel cell, J. Appl. Electrochem. 28(3) (1998) 289–297.

[6] K. Scott, W.M. Taama, P. Argyropoulos, Engineering aspects of the direct methanol fuel cell system, J. Power Sources, 1998.

[7] A.K. Shukla, P.A. Christensen, A.J. Dickinson, A. Hamnett, A liquid feed solid polymer electrolyte direct methanol fuel cell, J. Power Sources 76(1) (1998) 54–59.

[8] M.K. Ravikumar, Studies on Direct Methanol Fuel Cells and Nickel-Iron Batteries, Indian Institute of Science, 1996.

[9] A.S. Arico, A.K. Shukla, K.M. El-Khatib, P. Creti, V. Antonucci, Effect of carbon supported and unsupported Pt-Ru anodes on the performance of solid polymer electrolyte direct methanol fuel cells. J. Appl. Electrochem., 1998.

[10] A.S. Arico, P. Creti, P.L. Antonucci, J. Cho, H. Kim, V. Antonucci, Optimization of operating parameters of a direct methanol fuel cell and physico-chemical investigation of catalyst-electrolyte interface, Electrochimica Acta 43(24) (1998) 3719–3729.

[11] M. Hogarth, P. Christensen, A. Hamnett, A. Shukla, The design and construction of high performance direct methanol fuel cells 1. Liquid feed systems, J. Power Sources 69 (1997) 113–124.
[12] M.P. Hogarth, G.A. Hards, Direct methanol fuel cells. Technological advances and further requirements, Platinum Metals Review 40(4) (1996) 150–159.
[13] M.P. Hogarth, J. Munk, A.K. Shukla, A. Hamnett, Performance of a carbon-cloth bound porous-carbon electrodes containing an electro-deposited platinum catalyst towards the electrooxidation of the methanol in sulphuric acid electrolyte, J. Appl. Electrochem. 24 (1994) 85–88.
[14] J.T. Wang, J.S. Wasmus, R.F. Savinell, M. Litt, A direct methanol fuel cell using acid doped polybenzimidazole as polymer electrolyte, J. Appl. Electrochem. 26 (1996) 751–756.
[15] J.T. Wang, S. Wasmus, R.F. Savinell, Real time mass spectrometric study of the methanol crossover in a direct methanol fuel cell, J. Electrochem. Soc. 143(4) (1996) 1233–1239.
[16] K. Scott, W.M. Taama, P. Argyropoulos, Material aspects of the liquid feed direct methanol fuel cell. J. Appl. Electrochem., 1998.
[17] W.M. Taama, P. Argyropoulos, K. Scott, Parametric studies on the liquid feed DMFC. IChemE Research Event in Newcastle upon Tyne, 1998.